Design of High-Density Cable Parameters for Controlling Spatial-Mode Dispersion of Randomly Coupled Multi-Core Fibers

Yusuke Yamada, Taiji Sakamoto, Masaki Wada, Saki Nozoe, Yuto Sagae, Yoko Yamashita, Hisashi Izumita, *Member, IEEE*, Kazuhide Nakajima, *Member, IEEE*, and Hiroaki Tanioka

(Top-Scored Paper)

***Abstract*—In this work, we propose design parameters for optimized high-density optical cables to control the spatial-mode dispersion (SMD) of randomly coupled multi-core fibers (MCF). The analytical results of our proposed cable demonstrated the controllability of the bending and twisting of the implemented optical fibers by means of tension that is applied for a bundled fiber while keeping the sufficient reliability. An optical characterization showed that appropriate cabling parameters resulted in SMD controllability and a 47% reduction of the SMD coefficient while avoiding undesired loss increase. C-L band transmission experiments using our optical cable showed no degradation of the Q-factor or mode-dependent loss (MDL). Our proposed cable design is beneficial for achieving an SMD-managed large-capacity and long-haul transmission link.**

***Index Terms*—Optical fiber cable, randomly coupled multi-core fiber, spatial-mode dispersion.**

I. Introduction

MUTI-CORE fiber (MCF) is an ideal transmission medium for increasing the transmission capacity in a limited cabling space. MCF can be categorized as weakly or randomly coupled. Weakly coupled MCF is designed so that signals transmitted through each core have negligible inter-core crosstalk. This requires a relatively larger core pitch. Randomly coupled MCF is designed to form a super-mode by controlling the coupling condition of neighboring cores with a smaller core pitch. Thus, the coupled MCF intrinsically attains a higher spatial density [1], [2], although it needs multiple-input multiple-output (MIMO) equalizers. The management of spatial-mode dispersion (SMD) is important with randomly coupled MCF since it is closely related to the MIMO complexity and limitations in transmission distance. The SMD coefficient in a loose tube cable has been experimentally investigated [3], and the lowest SDM coefficient of 2.5 ps/$\sqrt{}$km was observed in an installed loose tube cable link [4]. However, other reports have shown that SMD highly depends on the bending and twisting conditions [5], [6]. Thus, it is important to clarify the effect of cabling parameters on SMD and to control its properties by optimizing the parameters.

Methods of controlling the state of optical fibers in an optical cable have contributed to improving polarization-mode dispersion (PMD) [7], [8]. These methods depend on the shape of the cable elements, e.g., the buffer-tube or slotted-rod cables. However, structural control of the cable elements results in less efficient use of space. We previously investigated an optical cable with bending and torsion controlled using a bundle tape in a high-density optical cable and demonstrated its feasibility and reduced SMD [9].

In this paper, we investigate the controllability of SMD with the proposed cabling parameters. First, we describe the bending and twisting model of an optical fiber based on the tension and pitch of optical cable structure parameters. We then quantitatively analyze the fabricated cable to clarify the cable parameter dependence of bending and the overall reliability of the fiber. Next, we describe the controllability of the SMD and the optimum cabling parameters derived from the optical characteristics. We then determine the controllability and optimum cabling parameters of the SMD on the basis of the optical characteristic evaluation results. We also report the transmission characteristics of the proposed the designed cable.

II. Optical Cable Structure Model and Cabling Parameters for Controlling SMD

Fig. 1 shows our model for controlling the bending and twisting conditions in a high-density optical cable using a partially bonded optical fiber ribbon. The cross-section of a 200-fiber cable is depicted in (a). Its basic structure is the same as that of the high-density cable already in practical use [10]. This cable is composed of fifty 4-fiber partially bonded ribbons, strength members, rip cords, and a polyethylene sheath. The longitudinal bonding dimension of the partially bonded ribbon is designed to ensure mass-splicing workability in the same way

Manuscript received July 15, 2020; revised October 16, 2020 and November 25, 2020; accepted December 3, 2020. Date of publication December 18, 2020; date of current version February 16, 2021. *(Corresponding author: Yusuke Yamada.)*

The authors are with NTT Access Networks Service Systems Laboratories, Tsukuba 305-0805, Japan (e-mail: yuusuke.yamada.ze@hco.ntt.co.jp; taiji.sakamoto.un@hco.ntt.co.jp; masaki.wada.ar@east.ntt.co.jp; saki.nozoe.dn@east.ntt.co.jp; yuuto.sagae.nm@hco.ntt.co.jp; youko.yamashita.ku@hco.ntt.co.jp; hisashi.izumita@ntt-at.co.jp; kazuhide.nakajima.gr@hco.ntt.co.jp; hiroaki.tanioka.nh@hco.ntt.co.jp).

Color versions of one or more of the figures in this article are available online at https://doi.org/10.1109/JLT.2020.3045761.

Digital Object Identifier 10.1109/JLT.2020.3045761

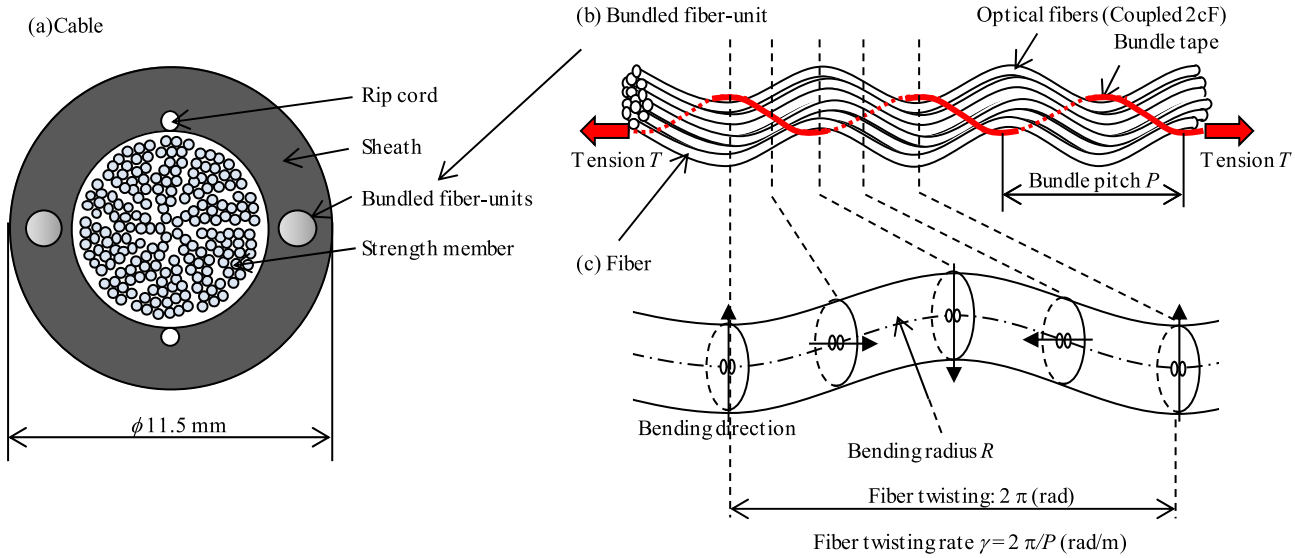

Fig. 1. Cabling parameters for controlling fiber bending and twisting.

as the practical partially bonded ribbon [10]. The cable has ten fiber-units containing five partially bonded optical fiber ribbons, and each unit is stranded. The outer diameter is 11.5 mm. The fiber density is 1.9 fiber/mm^2. Here, the structural feature of this optical cable is an optical fiber unit with intentional deformation. Fig. 1(b) shows a longitudinal image of a fiber unit bundled with tape (as shown by the red line). By winding the bundle tape around the fiber unit with bundle pitch P and tension T, the bundled optical fiber in the fiber unit is simultaneously deformed into a helical shape, as schematically shown Fig. 1(c). This deformation enables the bending radius R and twisting pitch γ to be varied. It was previously determined that the SMD coefficient of coupled MCF varies with R and γ [2]. As a result, we hypothesize that the SMD coefficient can be controlled in a high-density optical cable by optimizing P and T.

Fig. 2 shows the calculated R applied to the optical fiber in the bundled fiber unit. R value can be calculated as [11]

$$R = \left\{ r^2 + (P / 2\pi)^2 \right\} / P, \tag{1}$$

where r = (D-d) / 2 denotes a helical radius, and d and D are the fiber unit diameter and outer diameter of the deformed fiber unit, respectively, as shown in Fig. 2(a). R was calculated assuming that the optical fibers in the unit were ideal helices. D was directly measured with a micro gauge. The horizontal axis in Fig. 2(b) shows the relative value normalized with a value used in a conventional high-density cable. The green, red, and blue symbols indicate the results obtained when P was set to 30, 60, and 100 mm, respectively. Here, P = 30, 60, and 100 mm corresponds to the γ of 20 π, 33.3 π, and 66.7 π, respectively.

Fig. 2(b) shows the tendency of R to decrease and saturate to a particular level (indicated by the dash-dotted lines) when sufficient tension is applied. This is because the bundle tape is straightened at a larger tension and r value convergence to half of the fiber unit diameter d. The measured fiber unit diameter was d = 1.5 mm in our experiments. As a result, Fig. 2(b) supports the notion that R and γ in our fiber unit can be controlled with P and T.

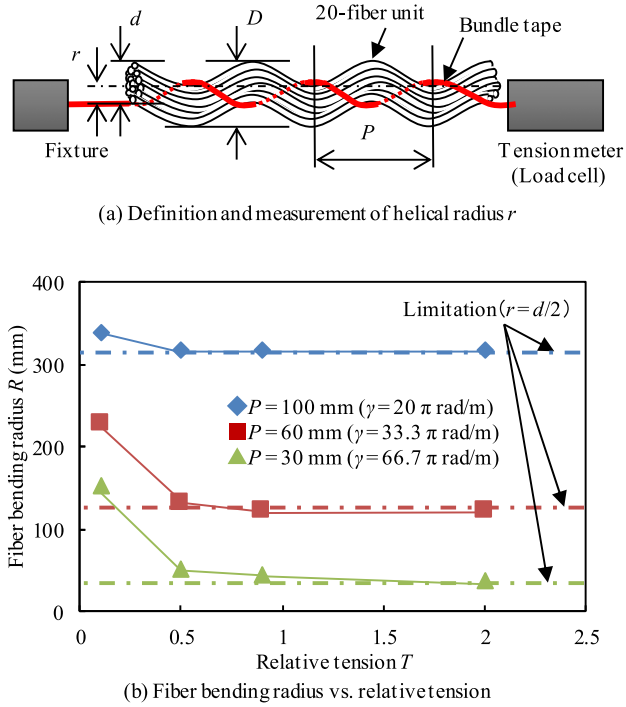

Fig. 2. Relationship between bundled fiber-unit parameters (P and T) and fiber bending radius R.

III. Experiments and Discussion

A. Fiber State Control in Optical Cables

We fabricated four 1.2-km-long 200-fiber cables with the structural parameters shown in Table I. Cable A is a typical high-density cable without intentional tension applied to the bundle

TABLE I
FABRICATED CABLING PARAMETERS

Cable ID	Number of fibers	Bundle pitch P (mm)	Tension T (Relative value)
A	200 fibers (2cF: 4 fibers)	60	< 0.3
B	200 fibers (2cF: 5 fibers)	60	0.5
C	200 fibers (2cF: 5 fibers)	60	1
D	200 fibers (2cF: 4 fibers)	60	2

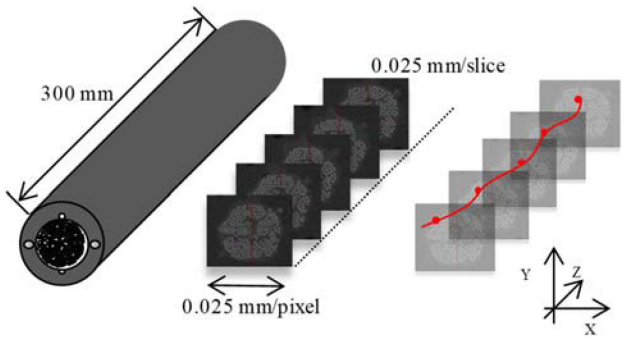

Fig. 3. Fiber locus measurement by X-ray CT.

tape. P was set to 60 mm as a constant, which is the typical pitch at which optical fibers are bundled, and the relative T was set to < 0.3, 0.5, 1.0, and 2.0 for cables A, B, C, and D, respectively. Here, T is a relative value based on the minimum controllable tension applied to the bundle tape during the cabling process. Sufficiently high tension (i.e., cable D) was also set because the intentional deformation may be hindered by high-density mounting in the optical cable. In order to verify fiber deformation in the fabricated cable, we measured the 3D-fiber-position using X-ray computed tomography (CT) images observed at a cable cross-section [12]. Fig. 3 shows the procedure for measuring the state of optical fibers in a cable and determining the locus of an optical fiber. In order to fix the fibers' positions during the CT measurement, we injected epoxy resin into the cable core. Once the resin hardened, we cut the cable of a 300-mm-long sample and measured the CT images, the results of which are shown in Fig. 3(a). The image resolution was 0.025 mm/pixel. Fig. 3(b) shows the measurement of the cross-sectional absorption coefficient image along with the sample.

Fig. 4 shows the measured locus of an optical fiber in the cables. Each graph shows the result measured in the orthogonal axis. The solid and dashed lines represent the measured result and the fitting curve based on the design value, respectively. Here, the fitting curve was fitted by a sine function on the assumption that the locus of the optical fiber was a helix. P_{fit} is the pitch of the helix as determined from the fitting curve of the measured result. In cable A, the pitch of the meander was found to be irregular and slightly deviated because the bundle tape loosely bundled the optical fibers. We can assume that the deformation of the entire structure into a large circular arc was caused by the stranding of the units. In cables B, C, and D, where $T = 0.5$ or higher, the optical fiber helically deformed as tension increased. Fig. 4(b), (c), and (d) shows that helical deformation was well maintained in the cabled fiber unit, and the measured P_{fit} values of 58.3–62.4 mm are in good agreement with the designed value of 60 mm. Here, the excess fiber length (*EFL*) in the cable is one of the design parameters that affects the cable performance [13]. Therefore, we estimate the *EFL* required for this cable structure, which can be calculated geometrically by

$$EFL = \sqrt{P^2 + (\pi d^2 / 4)^2}. \quad (2)$$

The helical diameter obtained from the amplitude of the optical fiber locus in Fig. 4(d) is $d = 0.2$ mm. The calculated EFL is 0.03%, which is sufficiently small compared to the *EFL* of 0.9% for conventional tube type cables [13]. We also investigated the relationship between curvature and tension in order to characterize the controllability of the bending state of the optical fiber in the cable. Fig. 5 shows the curvature distribution of the optical fiber. Here, the curvature was calculated from a circle passing through three adjacent points in the longitudinal direction. Fig. 5(a) shows the curvature distribution in the longitudinal direction obtained from the locus in the optical cable. The horizontal axis is the position in the longitudinal direction, and the vertical axis shows the curvature. The curvature is distributed in the range of 0.1–10 m^{-1}. Fig. 5(b) shows the curvature distribution of the fibers in the cable. The solid line shows the log-normal distribution curve. The median values of cables A, B, C, and D were 1.62, 1.47, 2.66, and 3.44, respectively. The curvature and dispersion of cable A were slightly large, which might be attributed to the large dispersion caused by the loose bundle. When $T = 0.5$ or higher, the curvature can be controlled as the tension increases.

In order to ensure the long-term reliability of optical cables, it is important to suppress the mechanical strain of the optical fibers. We measured the tension of the bundle tape and strain applied to the optical fiber. The strain was measured by Brillouin optical time domain reflectometry [14] over a total length of 1.2 km for each of the 30 single-core optical fibers installed in the cable. The filled circle in Fig. 6 shows the average value of measured strain. The effect of tension on the strain of the optical fiber was negligibly small, and the average and maximum at T = 2.0 were 0.007% and 0.017%, respectively. We also determined that the cabling residual strain was less than 0.03% [10], which is required for high-density optical cables, thus ensuring long-term reliability.

B. Optical Characteristics of Optical Fiber Cables

Next, we examined the optical properties of the fabricated cables. Fig. 7 shows the cabling loss increase (filled and open circles) and the SMD coefficient (triangles) measured at 1550 nm. Here, the cabling loss increase corresponds to the loss difference between cabled and uncabled optical fibers. The 2cF we used had a core pitch of 20 μm. Each core of the 2cF had a step index profile and the cutoff wavelength was 1435 nm. As

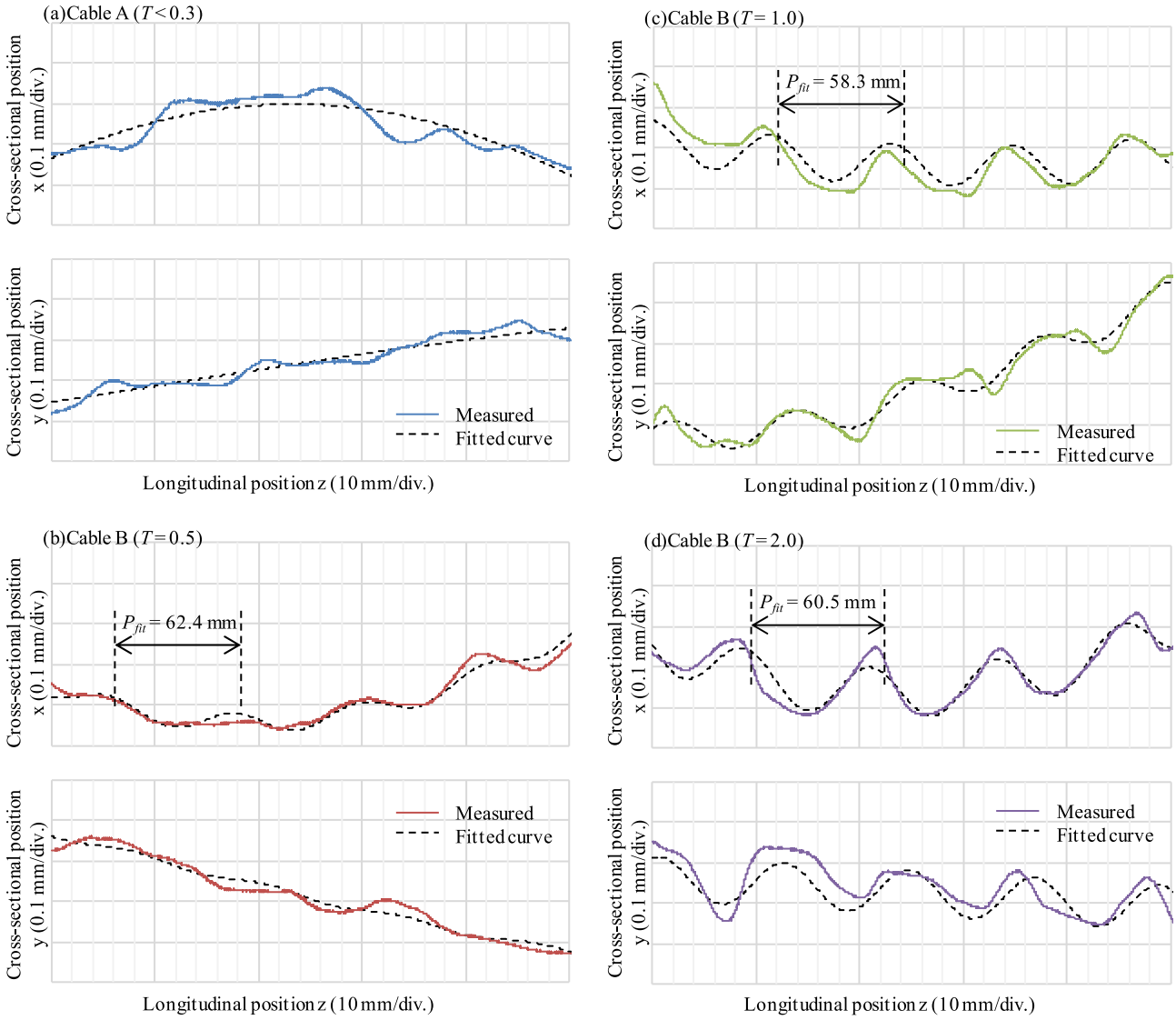

Fig. 4. Measured fiber locus in the fabricated cables.

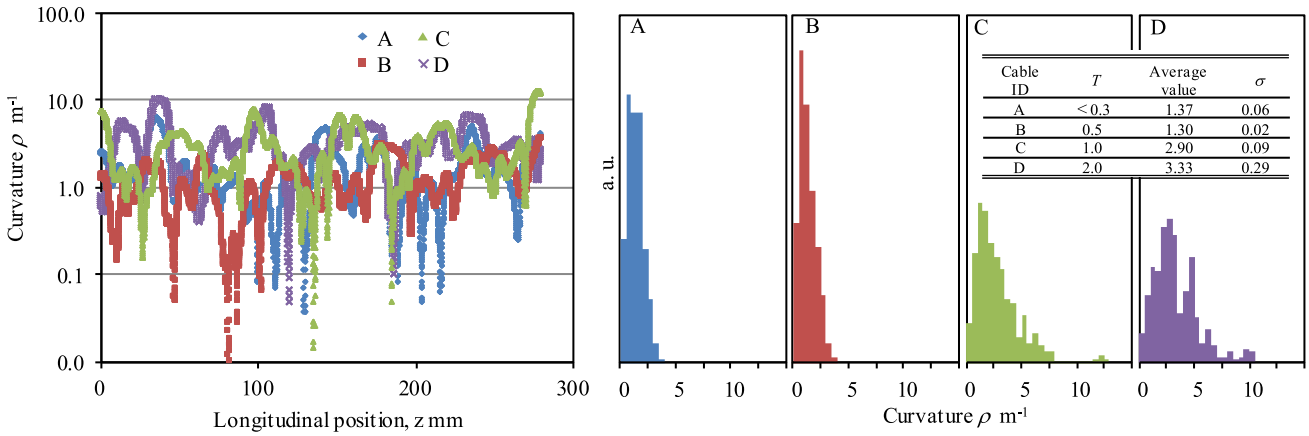

Cable ID	T	Average value	σ
A	< 0.3	1.37	0.06
B	0.5	1.30	0.02
C	1.0	2.90	0.09
D	2.0	3.33	0.29

(a) Curvature distribution along longitudinal position

(b) Probability distributions of curvature

Fig. 5. Cabled fiber curvature calculated from measured fiber locus.

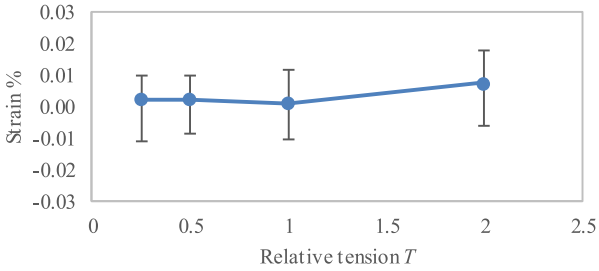

Fig. 6. Mechanical strain characteristics vs relative tension.

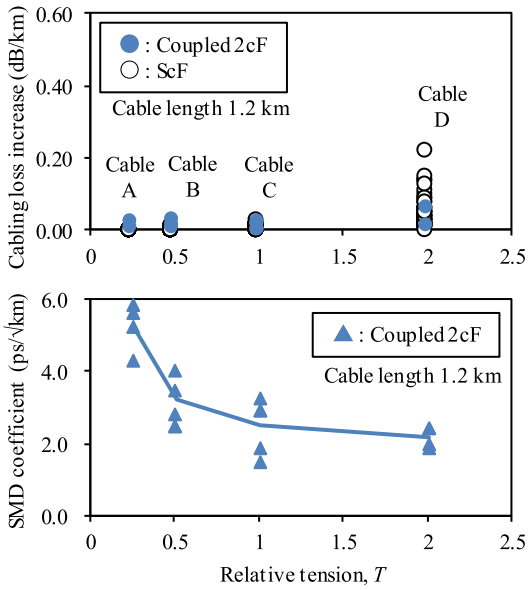

Fig. 7. Cabling loss increase and SMD coefficient as a function of relative tension measured at 1550 nm.

seen in Fig. 7, the loss of both 2cFs and ScFs degraded in cable D. A tension greater than the conventional high-density optical cable results in an increase in macro and/or micro bending loss.

Fig. 7 also shows that cables A, B, and C had no significant loss increase. The average optical loss of the coupled 2cFs assembled into cable C was 0.23 dB/km at 1550 nm and 0.22 dB/km at 1625 nm. For comparison, that of the ScFs was 0.19 dB/km at 1550 and 0.22 dB/km at 1625 nm. Thus, for the cabling loss increase of 2cF, we can expect a dependency on P and T similar to that in the conventional ScF. To determine the SMD coefficient, we used a conventional fixed analyzer method typically used for measuring PMD [15]. We derived the Fourier transformed data using the measured interference spectrum. As seen in Fig. 7, SMD coefficients tended to decrease as T increased. The average values of the SMD coefficients measured with cables A, B, C, and D (solid lines) were 5.3, 3.2, 2.5, and 2.2 ps/$\sqrt{}$km, respectively. We verified that cable C could reduce the SMD coefficient by 47% compared with cable A while retaining an acceptable cabling loss increase.

Fig. 8 shows the wavelength dependence of the SMD coefficient of cable C. Each plot shows the result obtained with a different 2cF in the cable. We verified that the SMD coefficients of five cabled 2cFs were successfully controlled in the wide wavelength range of 1530–1610 nm.

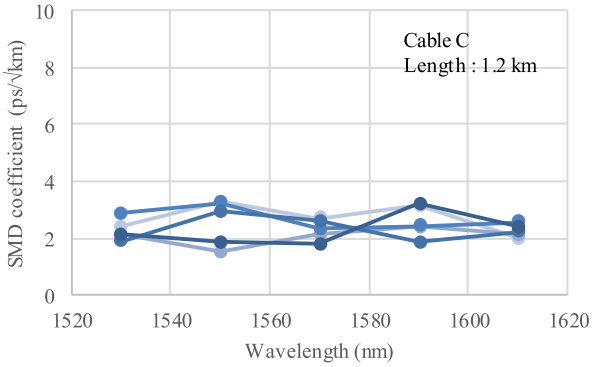

Fig. 8. Wavelength dependence ofSMD coefficients measured with cable C.

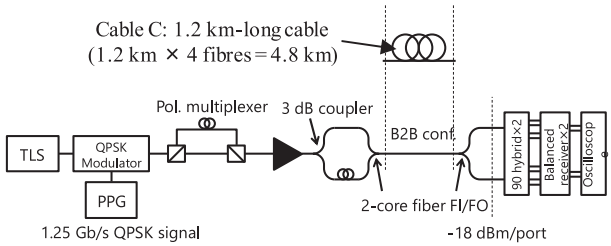

Fig. 9. Set-up for measuring the transmission characteristics.

TABLE II
TRANSMISSION CHARACTERISTICS

Wavelength nm	Q-factor dB		MDL dB		Penalty dB	
	B to B	Transmitted	B to B	Transmitted	Q penalty	MDL penalty
1530	14.6	14.4	1.1	1.2	0.2	0.1
1550	17.3	16.9	1.2	1.3	0.4	0.1
1565	16.4	16.8	1.0	1.1	-0.4	0.0
1600	15.6	15.5	1.1	1.1	0.1	0.0

In order to determine whether the transmission characteristics of the optical cable are sufficient in terms of the mode dependent loss (MDL) characteristic, the Q factors and MDL penalty of the transmitted signals were evaluated in the configuration shown in Fig. 9. Four 2cFs accommodated in cable C were connected in tandem for a total length of 4.8 km. A single-wavelength tunable laser source was used and the light was modulated into polarization-multiplexed 1.25 Gb/s QPSK signals. The signal was then split into two ports and decorrelated by the 100-m delay line. The signals were launched into two cores through the fan-in device. The transmitted signals were then demultiplexed by the fan-out device and detected by the MIMO receivers. The transmission wavelength was swept from 1530 to 1600 nm and the Q factors or MDL penalty of the signal at 1530, 1550, 1565, or 1600 was evaluated, respectively. The signal was recovered by 4 × 4 MIMO processing with the adaptive algorithm of IPNLMS. The equalizer length corresponded to a four-symbol period, which was sufficient given the bit-rate and SMD coefficient of the transmission setup. Table II shows the Q-factor measurements and mode-dependent loss (MDL) values between back-to-back and 4.8-km transmission. We observed that the Q-factor and MDL penalty were sufficiently small. The flat characteristic without wavelength dependence enabled

sufficient random coupling due to the effective contribution of bending by the bundle tape. These results demonstrate that the SMD coefficient of a coupled MCF can be controlled by appropriately setting high-density cabling parameters such as bundle pitch and tension.

IV. Conclusion

In this work, we investigated the controllability of SMD coefficients by designing appropriate optical cabling parameters. Our findings indicate that the bending and twisting of the optical fiber could be controlled by properly setting the tension T and bundle pitch P of the bundle tape. We verified that the curvature ρ derived from the analysis of the produced optical cable was distributed at less than 10 m^{-1} and correlated with tension T. We also determined that the mechanical strain applied to the optical fibers was sufficiently small and would ensure long-term reliability. Suitable T and P values enabled lower optical loss characteristics and controllability of the SMD coefficient, and the SMD coefficient was subsequently reduced by up to 47% in the fabricated cable. The optical cable demonstrated excellent characteristics in a transmission experiment at the wavelengths of 1530–1600 nm for 4.8 km. We believe that an optical cable with controlled SMD characteristics will greatly support future developments in SDM-based long-haul and large capacity transmission.

References

[1] T. Hayashi, Y. Tamura, T. Hasegawa, and T. Taru, "125-μm-cladding coupled multi-core fiber with ultra-low loss of 0.158 dB/km and record-low spatial mode dispersion of 6.1 ps/km1/2," in *Proc. 36th Opt. Fiber Commun. Conf.*, 2016, Paper Th5A.1.

[2] T. Sakamoto *et al.*, "Randomly coupled single-mode 12-core fiber with highest core density," in *Proc. 37th Opt. Fiber Commun. Conf.*, 2017, Paper Th1H1.

[3] T. Hayashi, T. Nagashima, T. Muramoto, F. Sato, and T. Nakanishi, "Spatial mode dispersion suppressed randomly coupled multi-core fiber in straightened loose-tube cable," in *Proc. 39th Opt. Fiber Commun. Conf.*, 2019, Paper Th4A.2.

[4] T. Hayashi *et al.*, "Field-Deployed multi-core fiber testbed," in *Proc. 24th OptoElectron. Commun. Conf. Int. Conf. Photon. Switching Comput.*, 2019, pp. 3.

[5] T. Hayashi, Y. Tamura, and T. Hasegawa, "Record-Low spatial mode dispersion and ultra-low loss coupled multi-core fiber for ultra-long-haul transmission," *J. Lightw. Technol.*, vol. 35, no. 3, pp. 450–457, 2017.

[6] S. Aozasa *et al.*, "Bending radius dependence of spatial mode dispersion in randomly coupled multi-core fiber," in *Proc. 37th Opt. Fiber Commun. Conf.*, 2017, Paper Th1H.4.

[7] L. F. Marques, A. M. Simiiio, and R. F. Cruz, "Statistical analyses of PMD using monte carlo method for different configuration of loose tube optical cable," in *Proc. 21st Opt. Fiber Commun. Conf.*, 2001, Paper WDD12-1.

[8] K. Toge and K. Hogari, "Effect of cabling on polarization mode dispersion in optical fiber ribbon cables," *Opt. Fiber Technol.*, vol. 14, pp. 149–153, 2008.

[9] Y. Yamada *et al.*, "Spatial mode dispersion control in a coupled MCF using high density cabling parameters," in *Proc. 40th Opt. Fiber Commun. Conf.*, 2020, Paper M4C.5.

[10] Y. Yamada *et al.*, "Development of novel optical fiber ribbon assembled into extremely high-density optical fiber cable," in *Proc. 61st Int. Cable Connectivity Symp. 2-2*, 2012, pp. 26–30.

[11] S. Stueflotten, "Design flexibility with loose tube fiber cables," in *Proc. 4th Annu. Eur. Fiber Opt. Commun. Local Area Netw. Expo. Int. Congrescentrum Rai*, 1986, pp. 12–15.

[12] M. Kikuchi, Y. Yamada, J. Kawataka, H. Izumita, and K. Katayama, "3-D measurement of rollable fiber ribbons in 1000-fiber cable and calculated fiber reliability," *Photon. Technol. Lett.*, vol. 30, no. 17, pp. 1519–1522, 2018.

[13] J. M. Regalado, A. Bertaina, and L. Provost, "Low-Attenuation and high excess-fiber length OPGW using G.652D bend insensitive fibers," in *Proc. 61st Int. Cable Connectivity Symp.*, 2012, pp. 329–334.

[14] T. Kurashima, T. Horiguchi, H. Izumita, S. Furukawa, and Y. Koyamada, "Brillouin optical-fiber time domain reflectometry," *IEICE Trans. Commun.*, vol. E76-B, no. 4, pp. 382–390, Apr. 1993.

[15] ITU-T Recommendation G.650.2, 2007.

Yusuke Yamada received the B.E. and M.E. degrees in environmental system engineering from the Nagaoka University of Technology, Niigata, Japan, in 2003 and 2005, respectively. In 2005, he joined NTT Access Network Service Systems Laboratories, Tsukuba, Japan, where his research focuses on optical fiber cable. He has contributed to the activity of IEC SC86B in 2013–2014 and IEC SC86A since 2017. He is currently a Senior Research Engineer with NTT Access Network Service Systems Laboratories. He was the recipient of the Best Paper Award at 12th OECC/IOOC in 2007. He is a member of the Institute of Electronics, Information, and Communication Engineers, Tokyo, Japan.

Taiji Sakamoto received the B.E., M.E., and Ph.D. degrees in electrical engineering from Osaka Prefecture University, Osaka, Japan, in 2004, 2006, and 2012, respectively. In 2006, he joined NTT Access Network Service Systems Laboratories, NTT, Tsukuba, Japan, where his research interests include optical fiber nonlinear effects, low nonlinear optical fiber, few-mode fiber, and multicore fiber for optical MIMO transmission systems. He is a member of the Institute of Electronics, Information, and Communication Engineers, Tokyo, Japan.

Masaki Wada received the B.E., M.E., and Ph.D. degrees from Hokkaido University, Hokkaido, Japan, in 2009, 2011, and 2018, respectively. In 2011, he joined NTT Access Network Service Systems Laboratories, NTT, Tsukuba, Japan, where his research interests include optical fiber design and optical amplifiers for space division multiplexing. He is currently a member of the Institute of Electronics, Information, and Communication Engineers, Tokyo, Japan.

Saki Nozoe received the B.E. and M.E. degrees in sustainable energy and environmental engineering from Osaka University, Osaka, Japan, in 2011 and 2013, respectively. In 2013, she joined NTT Access Network Service Systems Laboratories, NTT Corporation, Tsukuba, Japan. Her research focuses on the low-loss optical fiber design techniques. She is a member of the Institute of Electronics, Information, and Communication Engineers, Tokyo, Japan.

Yuto Sagae received the B.E. and M.E. degrees from Tohoku University, Miyagi, Japan, in 2013 and 2015, respectively. In 2015, he joined NTT Access Network Service Systems Laboratories, NTT, Tsukuba, Japan, where his research focuses on optical fiber designs. He is a member of the Institute of Electronics, Information, and Communication Engineers, Tokyo, Japan. He was the recipient of the Best Paper Award in OECC/PS 2019.

Yoko Yamashita received the B.S. and M.S. degrees in electronic engineering from Hokkaido University, Sapporo, Japan, in 2015 and 2017, respectively. Her research focuses on the modeling of planar lightwave circuit using the finite element method. She is a member of the Institute of Electronics, Information, and Communication Engineers, Tokyo, Japan.

Hisashi Izumita (Member, IEEE) joined NTT Transmission Systems Laboratories in 1989. He was engaged in the research on high-performance OTDR using coherent lightwave technologies and optical fiber distributed sensing applications. He also developed an optical fiber distribution system for central offices, an optical fiber maintenance and support system, and optical fiber cable. He has contributed to the activity of IEC TC86 WG4 and IEC SC86A WG1&WG3, in 1999 and 2012, respectively. He is currently a Senior Expert Engineer with NTT Advanced Technology Corporation. He is a member of OSA and the Japan Society of Applied Physics, and a Senior Member of IEICE.

Kazuhide Nakajima (Member, IEEE) received the M.S. and Ph.D. degrees in electrical engineering from Nihon University, Chiba, Japan, in 1994 and 2005, respectively. In 1994, he joined NTT Access Network Systems Laboratories, Tokai, Japan, where he was engaged in the research on optical fiber design and related measurement techniques. He is currently a Group Leader (Senior Distinguished Researcher) with NTT Access Network Service Systems Laboratories, Tsukuba, Japan. Since 2009, he has been a Rapporteur of Q5/SG15 of ITU-T. He is a member of the Optical Society, the Institute of Electronics, Information, and Communication Engineers, Tokyo, Japan, and the Japan Society of Applied Physics. He was the recipient of the Best Paper Award in OECC'96, the Best Paper Award in IEICE'11, the Achievement Award in IEICE'12, and the Maejima Hisoka Award in 2016.

Hiroaki Tanioka joined NTT in 1995. He has been currently engaged in the development of optical fiber cable. He is currently a Senior Research Engineer, Supervisor with NTT Access Network Service System Laboratories, Tsukuba, Japan.